Journal of Molecular and Cellular Cardiology 99 (2016) 57–64

Contents lists available at ScienceDirect

Journal of Molecular and Cellular Cardiology

journal homepage: www.elsevier.com/locate/yjmcc

Peptidase inhibitor 16 is a membrane-tethered regulator of chemerin processing in the myocardium

Michael Regn [a], Bernhard Laggerbauer [a], Claudia Jentzsch [a], Deepak Ramanujam [a], Andrea Ahles [a], Sonja Sichler [a], Julia Calzada-Wack [b], Rory R. Koenen [c], Attila Braun [d], Bernhard Nieswandt [d], Stefan Engelhardt [a,e,*]

[a] Institute of Pharmacology and Toxicology, Technische Universität München, Biedersteiner Straße 29, 80802 Munich, Germany
[b] Institute of Pathology, Helmholtz Center Munich, Ingolstädter Landstraße 1, 85764 Neuherberg, Germany
[c] Department of Biochemistry, Cardiovascular Research Institute Maastricht (CARIM), Maastricht University, Maastricht, The Netherlands
[d] Rudolf Virchow Center for Experimental Biomedicine, University of Würzburg, Josef-Schneider Straße 2, 97080 Würzburg, Germany
[e] DZHK (German Center for Cardiovascular Research) partner site Munich Heart Alliance, 80802 Munich, Germany

ARTICLE INFO

Article history:
Received 23 December 2015
Received in revised form 9 August 2016
Accepted 15 August 2016
Available online 15 August 2016

Keywords:
Peptidase inhibitor 16 (PI16)
Chemerin
RARRES2
TIG2
Protease inhibition
Chemerin processing

ABSTRACT

A key response of the myocardium to stress is the secretion of factors with paracrine or endocrine function. Intriguing in this respect is peptidase inhibitor 16 (PI16), a member of the CAP family of proteins which we found to be highly upregulated in cardiac disease. Up to this point, the mechanism of action and physiological function of PI16 remained elusive. Here, we show that PI16 is predominantly expressed by cardiac fibroblasts, which expose PI16 to the interstitium via a glycophosphatidylinositol (-GPI) membrane anchor. Based on a reported genetic association of PI16 and plasma levels of the chemokine chemerin, we investigated whether PI16 regulates post-translational processing of its precursor pro-chemerin. PI16-deficient mice were engineered and found to generate higher levels of processed chemerin than wildtype mice. Purified recombinant PI16 efficiently inhibited cathepsin K, a chemerin-activating protease, *in vitro*. Moreover, we show that conditioned medium from PI16-overexpressing cells impaired the activation of pro-chemerin. Together, our data indicate that PI16 suppresses chemerin activation in the myocardium and suggest that this circuit may be part of the cardiac stress response.

1. Introduction

Myocardial infarction, pressure overload or genetic defects of the cardiac muscle induce a pathologic response of the myocardium termed cardiac remodeling. It comprises fundamental changes in gene expression and the cellular and interstitial composition of the myocardium, among which cardiac myocyte growth (cardiac hypertrophy) and the deposition of extracellular matrix (cardiac fibrosis) are hallmarks. Cardiac remodeling involves intense intercellular communication, wherein secreted factors such as proteases, protease inhibitors, cytokines and chemokines [1] or nucleotides such as extracellular cAMP [2] serve a central role. Also, the invasion of immune cells into the impaired myocardium requires local expression of chemoattractant factors [3].

By screening a cardiac cDNA library for secreted proteins, we had previously identified peptidase inhibitor 16 (PI16) as a paracrine factor with potential cardiac function. Whereas basal cardiac expression of PI16 is low and much surpassed by that seen in other tissues [4], a dramatic upregulation was found during cardiac remodeling in animal disease models and humans [4]. Up to this point, PI16 had not revealed much of its function. One early observation about PI16 was its association with a serum peptide termed prostatic secretory protein 94 (PSP94) [5], which is consistent with the high expression of both binding partners in the prostate gland. The role of this association and the question in which tissue it is relevant, however, are elusive. Another finding that has not been understood yet is that PI16 has been found to specifically mark a subset of regulatory T cells (T_{reg}) [6,7].

Its peptide sequence classifies PI16 as a member of the CAP protein family, the functions of which appear to be diverse and largely not understood. PI16 (alias CRISP-9) has received its name from a sequence homology to peptidase inhibitor 15 (CRISP-8), which had been found to inhibit trypsin [8]. Whether PI16 likewise has peptidase-inhibiting activity remained unclear. C-terminal to the CAP domain of PI16 follows a long peptide sequence that is predicted to be unstructured and shares no obvious similarity to other proteins. PI16 appears in at least three electrophoretic isoforms, each corresponding to an apparent mass that is higher than its theoretical mass (74 kDa, 100 kDa and 108 kDa vs. 53 kDa). Glycosylation explains in part for the aberrant migration in

* Corresponding author at: Stefan Engelhardt, Institute of Pharmacology and Toxicology, Technische Universität München, Biedersteiner Strasse 29, 80802 Munich, Germany.
E-mail address: stefan.engelhardt@tum.de (S. Engelhardt).

http://dx.doi.org/10.1016/j.yjmcc.2016.08.010

gels, but not for the co-existence of these isoforms per se (deglycosylation shifts all three bands to faster-migrating forms without resolving them, see [4]). Thus, it was unclear how these isoforms are formed, where they localize to, and with which proteins they interact.

An intriguing perspective on the function of PI16 came from a genome-wide assocation study (GWAS) that identified potential regulators of chemerin levels. This study revealed correlation between a single nucleotide polymorphism (SNP) affecting the CAP-domain of PI16 (rs1405069) and elevated chemerin plasma levels [9]. Chemerin (alias retinoic acid receptor responder (tazarotene induced) 2, *RARRES2* or tazarotene induced gene 2, *TIG2*) is a ligand of chemokine-like receptor 1 (CMKLR1), G protein-coupled receptor 1 (GPR1) and chemokine receptor-like 2 (CCRL2), but only CMKLR1 appears to be activated by chemerin binding [10]. Chemerin exists in various isoforms that are generated by proteolytic cleavage of pro-chemerin. Several proteases have been shown to catalyze this activating step, whereas others were found to inactivate chemerin [10,11]. A synthetic peptide that had been delineated from chemerin (but does not seem to occur in nature) was found to be immunosuppressive and had been envisaged as a potential anti-inflammatory therapeutic. Two of the three chemerin receptors, GPR1 and CCRL2, appear to be silent receptors with presumed decoy function [12,13]. These findings in sum support the idea that chemerin may have both, pro- and anti-inflammatory functions. With respect to cardiac function, the pro-inflammatory CMKLR1 receptor is expressed by cardiac cells [14] and chemerin serum levels seem to correlate with dilated cardiomyopathy [15]. Together, these findings underscore the possibility that PI16 and chemerin are functionally coupled in the heart.

In this study, we asked whether peptidase inhibitor 16 (PI16) has a function in chemokine regulation in myocardium. We pursued this hypothesis by analyzing the expression of PI16, its association with and the processing of chemerin in wildtype and PI16-deficient mice, and tested for the impact of PI16 on chemerin receptor activation. Our data show that PI16 represses posttranslational processing of pro-chemerin, thereby controlling chemerin levels and signaling in the myocardium.

2. Results

2.1. PI16 is secreted by cardiac fibroblasts and tethers to their membrane via a GPI anchor

To approach the cardiac function of PI16, we generated a mouse line that is globally deficient of the PI16 gene. A PCR product was amplified that comprised neomycin cDNA with flanking frt sites, upstream of murine PI16 exons 3 to 4, and further framed by loxP sites. This product was cloned into a targeting vector for the transfection of mouse embryonic stem cells, and neomycin was used for selection. $PI16^{floxneo}$ mice carrying this insert were then crossed with a mouse line that encodes Flp recombinase to delete the neomycin cassette, and genetically confirmed offspring were then crossed with transgenic mice that express Cre recombinase under the control of the nestin promoter. The $PI16^{-/-}$ genotype (due to deletion of exons 3 to 4) was confirmed by Southern blotting (Fig. A.1). Under conditions that provoke strong upregulation of PI16 in wildtype mice, e.g. transverse aortic constriction (TAC), the $Pi16^{-/-}$×mice were still devoid of the protein (Fig. 1A), thus further confirming successful genetic deletion.

$PI16^{-/-}$ mice did not display an obvious phenotype under basal conditions, as litter size, gender distribution and also basal blood parameters (recorded 1, 3, 5 and 8 months after birth) were similar to wildtype controls (Fig. A.2 and Table A). Furthermore, analysis of the ratio between heart weight and body weight (HW/BW) and the extent of extracellular matrix formed were not changed in 8 months-old $PI16^{-/-}$ mice compared to controls, indicating that neighter cardiac hypertrophy nor fibrosis were induced by the absence of PI16 under basal conditions (Fig. A.3). Remarkably, application of TAC to $PI16^{-/-}$ mice likewise did not confer a phenotype within 28 d after surgery, as judged from the abovementioned parameters and from additional criteria for myocardial morphology and function (Fig. A.4). This finding was somewhat suprising in view of the strong upregulation of PI16 expression in this disease model. It is possible that constitutive deletion of the PI16 gene provokes compensatory expression of other genes, as has been observed in many cases [16]. It is also possible that the TAC model may not fully address the function of PI16 (see discussion).

To further approach the function of secreted PI16, we investigated where the protein localizes within the myocardium. Stainings of left ventricular sections revealed islet-like deposits in the interstitial extracellular space, which increased in number and size under TAC (Fig. 1B). We then asked whether cardiac cells endogenously express PI16 and, if so, in which of these it predominates. For this, we collected cells from left ventricular tissue of wildtype mice by Langendorff perfusion, sorted them by FACS for the presence of specific surface markers, and quantified PI16 mRNA therein by qPCR. This approach identified the cardiac fibroblast ($PDGFR^{+}$ cells) as the main source of intramyocardial PI16, whereas 6- to 11-fold lower levels were found in cardiac myocytes, leukocytes ($CD45^{+}$ cells), endothelial cells ($CD105^{+}$ cells) and others (Fig. 1C). Thus, although PI16 exists in cardiac myocytes and, as reported earlier [4], is able to modulate their hypertrophic response in vitro, the dominant cardiac function of PI16 may originate from the cardiac fibroblast.

Remarkably, bioinformatic analysis (http://mendel.imp.ac.at/sat/gpi; [17]) predicts the presence of a glycophosphatidylinositol- (GPI)-anchor attachment site at position 466 of the primary 489 residues-long murine PI16 protein (Fig. 1D). As GPI anchoring sites are determined by sequence context rather than by a specific consensus motif, their recognition requires complex algorithms and necessitates experimental validation. First experimental support for the GPI anchor in PI16 came from our finding that overexpression of PI16 in CHO cells enhanced detection of the protein on the cell membrane (Fig. B.1). To validate this further, cells were incubated with phospholipase C (PLC) to cleave PI16 at the GPI anchor. HEK293 cells, transiently transfected with a PI16 expression construct, were incubated in the presence or absence of PLC. Afterwards, cell-free supernatant was collected, cells were washed, and the fractions analysed by Western blotting using an anti-PI16 antibody. Conditioned medium from non-digested cells was loaded as a control. The analysis showed that the lysate of PLC-treated cells was devoid of PI16-bands that correspond to higher molecular mass, in favor of a band that appeared in the supernatant of these cells and corresponded to the main band observed in conditioned medium of control cells (Fig. 1E). In analogy to the effects exerted by PLC, deletion of the sequence that determines GPI-anchoring of PI16 (peptide positions 466–489) resulted in a pronounced PI16 band in the culture supernatant (Fig. B.2). Together, these data provide evidence for a functional GPI anchor that tethers PI16 to the cell membrane.

2.2. Secreted PI16 interacts with the chemokine chemerin

The intriguing genomic association between PI16 and chemerin [9], together with our experimental data on PI16, led us to ask whether chemerin is present in cardiac tissue and, if so, whether it is physically associated with PI16. Quantitative PCR analysis in FACS-sorted cells from mouse myocardium indeed showed an expression pattern of chemerin (*RARRES2*) similar to that observed for PI16, i.e. more prominent expression in cardiac fibroblasts than in the other cell types analysed (Fig. 2A). Consistent with the proposed function of chemerin, leukocytes also exhibited pronounced chemerin expression, yet to much lower extent than in cardiac fibroblasts (Fig. 2A).

Next, endogenous PI16 was immunoprecipitated using specific antibodies, immobilized on protein A resin, and analysed on blots using specific antibodies for PI16 and chemerin, respectively. Indeed, both

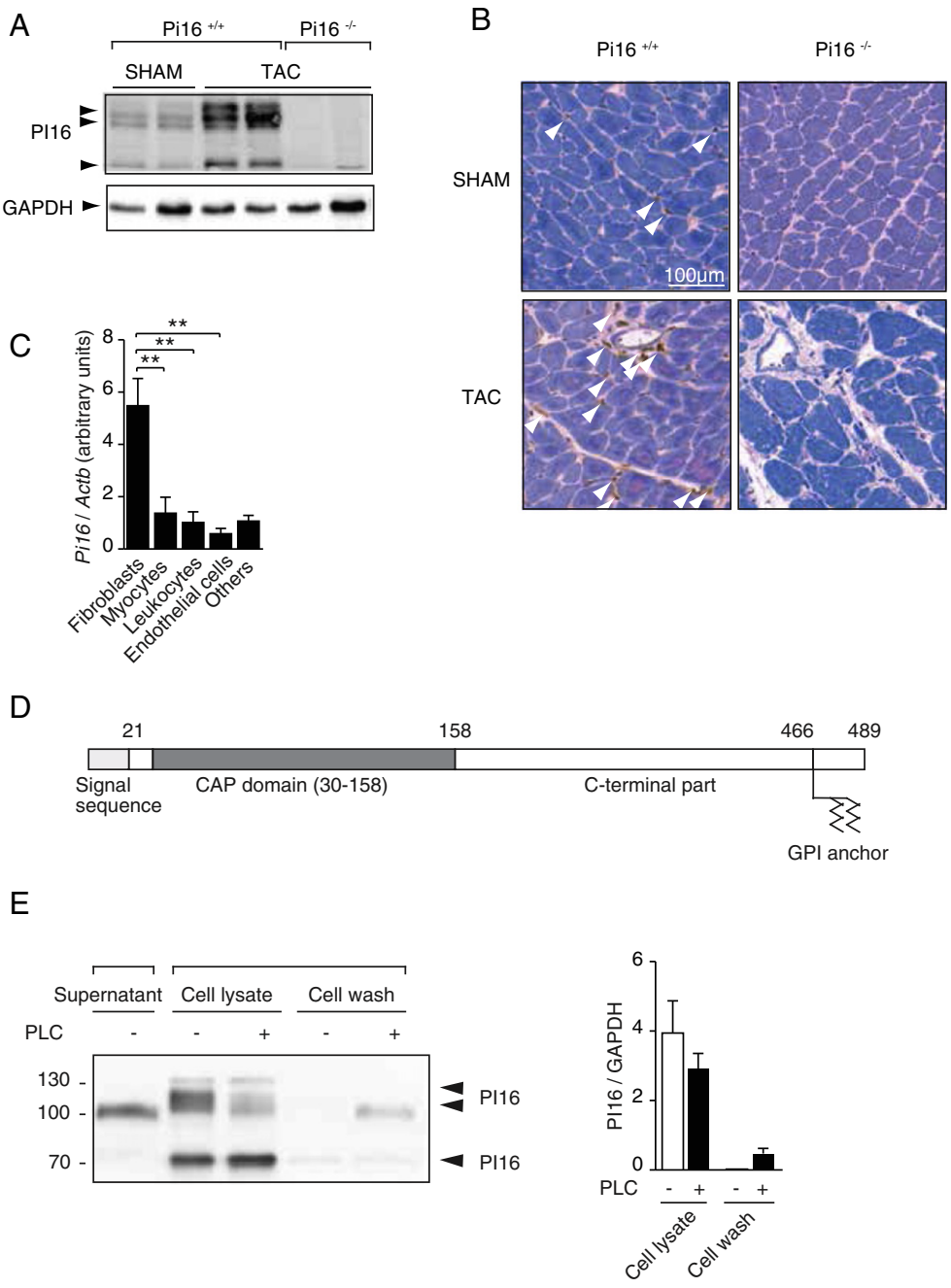

Fig. 1. PI16 is secreted by cardiac fibroblasts and tethers to their membrane via a GPI anchor. (A) Western blot analysis of PI16 in mouse myocardial tissue lysates, confirming TAC-induced upregulation of PI16 in wildtype mice ($PI16^{+/+}$) and global Pi16 deficiency in offspring from $PI16^{-/-}$ × Cre crossings. GAPDH detection served as loading control. Arrows indicate previously described PI16 variants. (B) Immunohistochemical staining of PI16 and Gomori-Masson counterstaining in myocardium from wildtype ($PI16^{+/+}$) or $PI16^{-/-}$ mice, subjected to transverse aortic constriction (TAC). Sham-operated mice served as controls. (C) Quantitative PCR analysis of *Pi16* mRNA in FACS-isolated primary cells from myocardium (fibroblasts sorted for PDGFRa, leukocytes for CD45, endothelial cells for CD105). Cells that were not positive for these markers were assigned as others. Myocytes were separated ahead of FACS by centrifugation ($n = 4$–7). Data are mean ± s.e.m. and are analysed using 1-way ANOVA with Bonferroni post-test. (D) Schematic structure of murine PI16, highlighting the CAP domain and the predicted GPI anchor attachment site, followed by a hydrophobic co-determinant of the anchor motif. (E) Immunoblot analysis for PI16 after phospholipase C (PLC) cleavage of the GPI anchor, demonstrating functionality of the latter. PI16 from lysed cells and cell-free supernatant was normalized to GAPDH ($n = 4$).

proteins were pulled down by the *anti*-PI16-antibody, whereas the negative control only showed a faint chemerin band (Fig. 2B). Consistently, transfection of HEK293 cells with plasmid constructs for murine full-length PI16 and pro-chemerin ($mChem^{162}$) allowed for efficient co-immunoprecipitation of both proteins (Fig. 2C).

Elevation of chemerin in humans, due to a SNP in the PI16 gene [9], prompted us to ask whether genetic deletion of PI16 in mice would alter the level of chemerin. Indeed, we found total chemerin protein 29% lower in PI16-deficient mice than in corresponding littermate controls (Fig. 2D). Since this ELISA could not discriminate between pro-chemerin and its processed forms, we fractionated myocardial cell lysates from wildtype and $PI16^{-/-}$ mice by SDS-PAGE and tested for chemerin on Western blots. A band that corresponds to the product(s) of pro-chemerin processing appeared more prominent in lysates from $PI16^{-/-}$ background than in wildtype (Fig. 2E). Of note, we also observed this impact on chemerin processing in adipose tissue (Fig. C), which naturally strongly expresses chemerin [18] and PI16 [4] and which is thought to be a site of chemerin function, too. Together, these

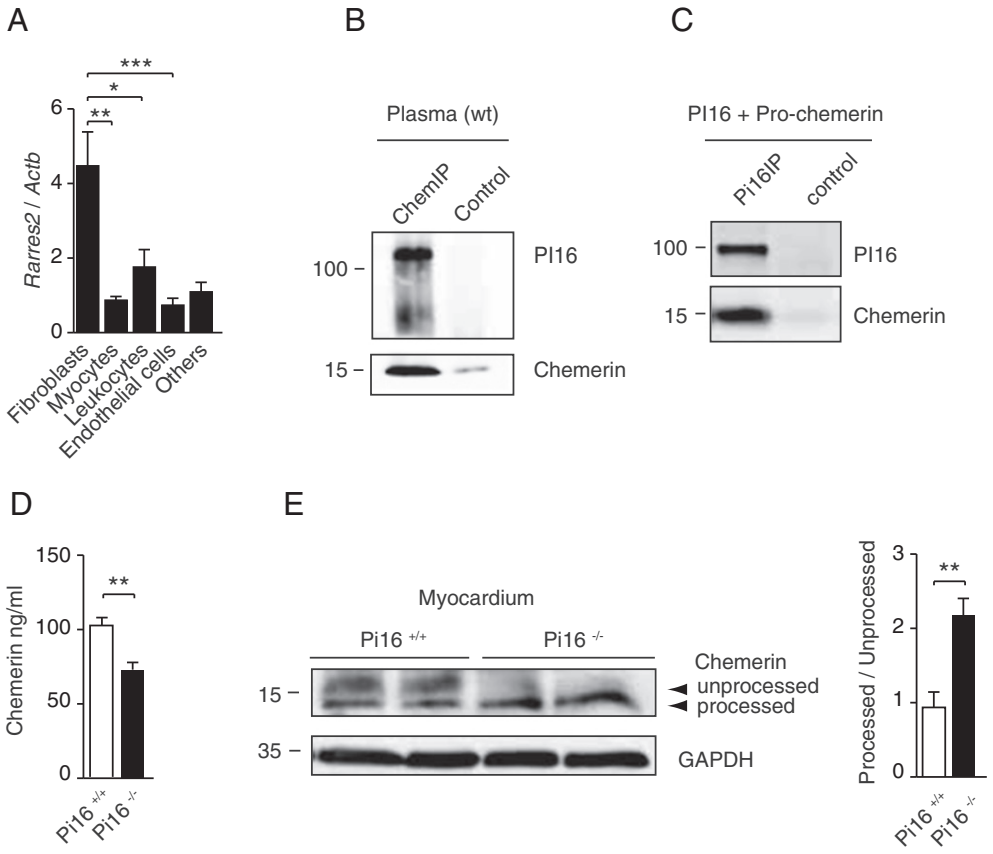

Fig. 2. Secreted PI16 interacts with the chemokine chemerin. (A) Quantitative PCR analysis of chemerin (*RARRES2*) mRNA in FACS-isolated primary cardiac myocytes, cardiac fibroblasts, leukocytes, endothelial cells and others from myocardium ($n = 2$–4). Data are mean ± s.e.m. and are analysed using 1-way ANOVA with Bonferroni post-test. (B) Pulldown of chemerin from plasma of wildtype mice, followed by immunoblot detection of PI16 and chemerin. Control IP without chemerin-antibody (control). (C) Pulldown of PI16 with anti-PI16 antibody from the cell culture supernatant of transiently transfected HEK293-cells with PI16 and pro-chemerin. Control denotes an IP without anti-PI16 antibody. (D) ELISA for total chemerin in plasma of $PI16^{+/+}$ and $PI16^{-/-}$ mice ($n = 7$–8). Data are mean ± s.e.m. and are analysed using unpaired *t*-test. (E) Analysis of chemerin-processing products in myocardium by immunoblot of chemerin in $PI16^{+/+}$ and $PI16^{-/-}$ mice. Quantification of processed and unprocessed chemerin variants (marked with arrows), shown as ratio of both ($n = 6$–7). Data are mean ± s.e.m. and are analysed using unpaired *t*-test.

data strengthen the idea that PI16 is physically and functionally associated with chemerin.

2.3. PI16 inhibits the (pro-)chemerin-processing protease cathepsin K

To test for the suspected protease-inhibiting function of PI16, two different experimental strategies were applied, using the PI16 constructs depicted in Fig. 3A. First, we analysed whether purified PI16 interfered with the activity of cathepsin K, a natural chemerin-activating protease [19]. CHO cells were stably transfected with a construct for the expression of a PI16 variant that lacked the GPI-anchoring motif (PI16-ΔGPI-Fc), but was expressed in fusion to a human IgG Fc sequence. PI16 was isolated from cell culture supernatant upon binding to protein A resin, eluted by glycine pH shock (assuming that the large fraction of cysteines preserves structure and activity of PI16) and afterwards buffered to pH 7.

Addition of purified PI16 to a colorimetric assay for cathepsin K activity revealed dose-dependent inibition of cathepsin K. In this assay, 0.3 μg PI16 achieved inhibition of cathepsin K, as seen also with the synthetic cysteine protease inhibitor E-64 (Fig. 3B). A 10-fold larger amount of purified Fc fragment, used as a negative control, had only little effect on the assay (Fig. 3B).

2.4. PI16 suppresses chemerin-dependent activation of the chemokine receptor CMKLR1

The second approach we devised is based on the rationale that secreted PI16 would be able to condition a culture medium such that it blocks the processing of pro-chemerin and thereby reduces the extent of chemerin-dependent receptor activation. As a readout for the latter, we measured β-arrestin2 recruitment by the chemerin receptor using fluorescence resonance energy transfer (FRET) (see Fig. 3C for experimental principle). HEK293-cells were transfected with two constructs encoding murine pro-chemerin and PI16-ΔGPI-Fc, respectively, and, the cell-free supernatant was transferred after 48 h to sensor cells that had been transfected with CMKLR1-CFP and a β-Arrestin2-YFP-fusion construct. Both fluorophores were expressed in their expected compartments (Fig. 3C) and ligand-dependent YFP-β-Arrestin2 recruitment to CMKLR1 was well detectable (documented by normalized FRET ratio YFP_{535}/CFP_{480}) (Fig. 3D). Importantly, supernatant from donor cells co-transfected with PI16 (next to pro-chemerin) significantly reduced CMKLR1 activation in sensor cells (Fig. 3E). Thus, both experimental strategies support the conclusion that PI16, by inhibiting proteolytic activation of pro-chemerin, obstructs signaling of this chemokine to other cells. We believe that the PI16-chemerin-CMKLR1-axis is a self-sufficient entity in the myocardium, which prevents overshooting of chemerin-induced responses in the injured myocardium. Examination of this scenario should be subject to upcoming studies.

3. Conclusions and discussion

In this study, we characterized PI16, a protein that is strongly upregulated in diseased myocardium. We provide evidence for PI16 secretion by cardiac fibroblasts, its extracellular tethering to their membrane, and its ability to inhibit proteolytic activation of the chemokine chemerin.

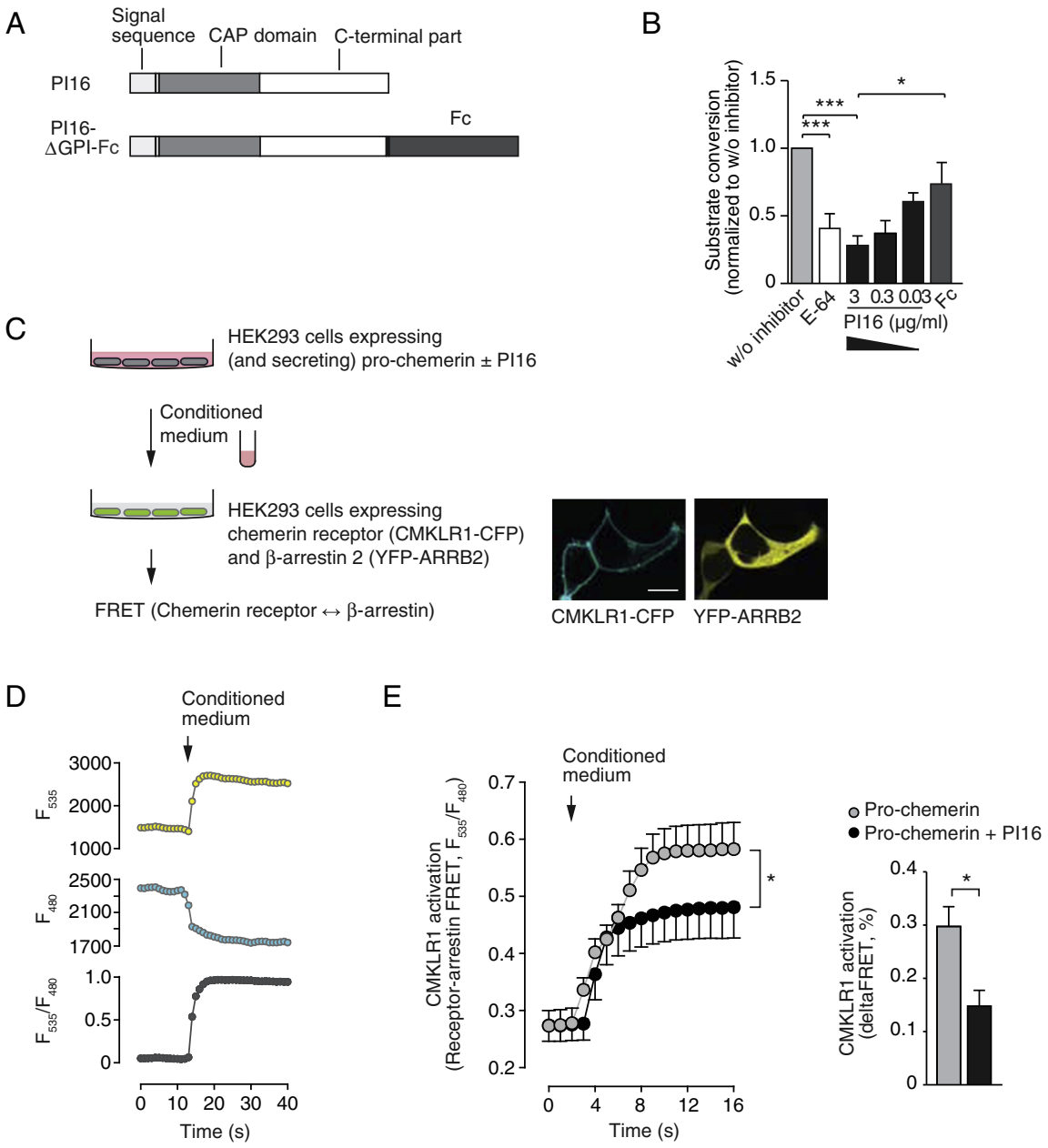

Fig. 3. PI16 inhibits processing of pro-chemerin, thereby reducing chemerin-dependent activation of the chemokine receptor CMKLR1. (A) Schematic illustration of PI16 constructs used for expression, purification and protease inhibition assays in comparison to murine PI16 (PI16). PI16-ΔGPI-Fc represents a truncated PI16 form that lacks the GPI-anchoring sequence. Fc designates a human IgG Fc sequence which was fused to PI16. (B) *In vitro* protease assay with cathepsin K and *Z*-Gly-Pro-Arg-AMC as a substrate. Bar 1 represents the substrate cleavage by cathepsin K in the absence of inhibitor. As a positive control for protease inhibition, cysteine protease inhibitor E-64 (0.1 mM) was added. Bars 3 to 5 show different concentrations of purified PI16-ΔGPI-Fc protein (3–0.03 µg/ml). The last bar on the right represents purified Fc alone ($n = 7$–8). Data are presented as mean ± s.e.m. and are analysed using 1-way ANOVA with Bonferroni post test. (C) Schematic illustration of the chemerin receptor-activation assay principle and localization of the chemerin receptor CMKLR1-CFP and β-Arrestin 2 (YFP-ARRB2) in chemerin receptor-sensor cells (scale bar: 10 µm). (D) Representative tracings of YFP (F_{535}) and CFP (F_{480}) emission intensities the FRET ratio F_{535}/F_{480}, recorded in a chemerin sensor cell after addition of conditioned medium. (E) *Left*, Time-dependent FRET ratio change in chemerin sensor cells that were stimulated with conditioned medium containing pro-chemerin or prochemerin + PI16-ΔGPI-Fc (mean ± s.e.m., $n = 9$). *Right*, FRET ratio change upon stimulation ($n = 14$–17). Data were analysed using multiple *t*-test (*$p < 0.05$).

Supported by genetic evidence that suggested a link between PI16 and chemerin, our data indicate that the myocardium is a self-sufficient entity for PI16-regulated processing of chemerin and that this circuit may be important in cardiac disease. We propose a model (Fig. 4) in which cardiac fibroblasts express PI16 and present it to the extracellular space through the GPI anchor moiety. As reported for many other proteins, this anchoring may be an intermediate step before PI16 is liberated by phospholipase activity. PI16 inhibits proteolytic processing of pro-chemerin, thereby preventing its activation. Through this mechanism, less chemerin is available to activate the receptor CMKLR1, which engages signaling towards chemotaxis [10]. Interference with chemerin signaling by PI16 should thus lead to reduced pro-inflammatory activation of leukocytes.

We do, at present, not know which of the processed chemerin variants is elevated in PI16-deficient mice, since the similar masses of these variants obstruct a differentiating analysis. The ability of PI16 to prevent chemerin-dependent CMKLR1 receptor activation argues in favor of the idea that PI16 inhibits the formation of active chemerin variants (corresponding to human Chem^{158}, Chem^{157} and/or Chem^{156}). In line with this, recombinant PI16 inhibited cathepsin K, a protease that activates

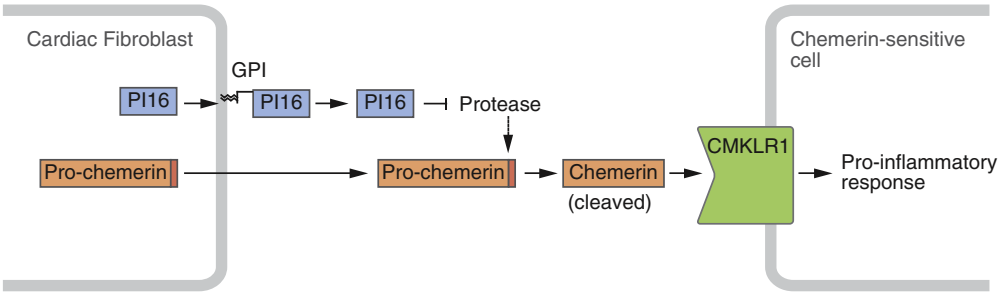

Fig. 4. Schematic model, illustrating the proposed role of PI16 in cardiac chemokine signaling: PI16 and pro-chemerin are expressed and secreted by cardiac fibroblasts. PI16 tethers to its expressing cell via its GPI anchor. In the interstitium, secreted PI16 inhibits proteolytic activation of (pro-)chemerin and thereby prevents chemerin-dependent activation of the G protein-coupled receptor CMKLR1 and subsequent pro-inflammatory pathways.

chemerin. Alternatively, however, PI16 could interfere with those proteases that inactivate chemerin [12], thereby raising the level of active chemerin. Interestingly elafin, an endogenous inhibitor of elastase (which, among other substrates, also processes pro-chemerin), has been related to cardiac injury after myocardial ischemia [20]. This emphasizes how profound the impact of endogenous peptidase inhibitors on cardiac function may be.

An important issue that future studies need to resolve is under which conditions PI16 upregulation modulates immune cell recruitment by chemerin. This may also explain why PI16 deficiency did not alter the response to TAC, but leaves open why wildtype mice upregulate PI16 in this disease setting. Our experimental model of transverse aortic constriction, which boosts PI16 expression, did not resolve this question, since these disease conditions favor cardiac remodeling rather than inflammation. Other than observed for PI16, TAC conditions do not seem to alter chemerin gene expression (data not shown). Interestingly, chemerin levels had recently been found to be elevated in heart failure patients [15]. It thus seems possible that certain cardiac conditions will reveal a pathologic interdependence of PI16 and chemerin.

Chemerin is expressed in many tissues, with adipose tissue, adrenal gland, liver, pancreas and reproductive system ranking high (www.ensembl.org). As a ligand of the chemokine receptor CMKLR1, chemerin is able to recruit macrophages and dendritic cells to adipose tissue [21]. Although the chemoattractant role of chemerin stands without doubt, other studies also suggested functions in fatty acid metabolism and glucose homeostasis, i.e. key aspects of the metabolic syndrome [10,11,22]. Chemerin-deficient mice are asymptomatic, but they show elevated blood glucose and impaired insulin regulation. These mice were also reported to have higher serum levels of non-esterized fatty acids, consistent with a role in lipolysis. High expression of chemerin in adipose tissue parallels intriguingly the high basal expression of PI16 in fat cells. Interestingly, the role of epicardial adipose tissue in cardiac disease is increasingly appreciated [23]. It would thus not be surprising if, in addition to a direct intramyocardial axis between PI16 and chemerin, both would also influence cardiac function through their activities in epicardial fat tissue. We believe that the data presented here provide a basis to pursue this hypothesis.

4. Materials and methods

4.1. Quantitative real-time PCR

Total RNA was prepared using PeqGOLD RNApure (Peqlab) according to the manufacturer's protocol. 500 ng RNA were reverse-transcribed using the Protoscript II cDNA Synthesis Kit (NEB, procedure according to manufacturer's protocol). Quantitative PCR analysis was conducted using the Fast Start SybrGreen MasterMix according to the standard protocol (Roche). The dissociation curve of the primers was monitored to control for primer specificity. Sample volume was 12.5 μl, containing 6.25 μl SybrGreen MasterMix, 400 pM primers and 10 ng template DNA. Primer sequences for real-time PCR were (gene symbols and species followed by sequences of forward and reverse primers):

Pi16 forward: 5′-CCAGTGCCCTCTTGGCTAC-3′
Pi16 reverse: 5′-ACCTCGGTCACCCTTGGA-3′
RARRES2 (chemerin) forward: 5′-GTGCACAATCAAACCAAACG-3′
RARRES2 reverse: 5′-GGCAAACTGTCCAGGTAGGA-3′
Actb forward: 5′-GCAGCTCCTTCGTTGCCGGT-3′
Actb reverse: 5′-TACAGCCCGGGGAGCATCGT-3′.

4.2. Cloning of plasmid vectors for expression

For expression in HEK293 and CHO cells murine Pi16 and murine pro-chemerin cDNAs were cloned into the pT-Rex-DEST 30 vector (Invitrogen). For fusion of the murine Pi16 sequence to hIgG1-Fc, the pFUSE-hIgG1-Fc vector (InvivoGen) was used. Pi16 was amplified by PCR with the following primers to delete the GPI-attachment site at the C-terminus and insert a tobacco etch virus protease cleavage site.

Pi16 forward: 5′-AAAAAAGGCGCCCGAGCCCATCAACAAGTTTG-3′.
Pi16 reverse: 5′-AAAAAAGCTCGAGATCGATTGGAAGTAGAGGTTCT CCTTCAAATCCCAGTCGGCC-3′.

4.3. Preparation of primary cardiac cells from mice, and FACS procedure

Cells were isolated from wildtype ($PI16^{+/+}$) and $PI16^{-/-}$ mice as described earlier [2]. In brief, hearts were explanted and perfused in buffer A (113 mM NaCl, 4.7 mM KCl, 0.6 mM KH_2PO_4, 0.6 mM Na_2HPO_4, 1.2 mM $MgSO_4$, 12 mM $NaHCO_3$, 10 mM $KHCO_3$, 10 mM HEPES, 32 μM Phenol Red, 30 mM taurine) in the presence of collagenase II. After dissociation and mechanical distortion of the tissue, cardiac myocytes were allowed to settle, before the pellet was resuspended in buffer B (47.5 ml of buffer A, 2.5 ml FCS, 10 mM $CaCl_2$). After 10 min sedimentation non-myocyte cells were pelleted from the supernatant and then staining with different cell type specific surface markers for cell sorting (CD45 for leukocytes, CD105 for endothelial cells, PDGFRa for fibroblasts) was performed. FACS was performed using a BioRad S3 cell sorter. The isolated cells were then cryoconserved at −80 °C and RNA-isolation followed as described above.

4.4. Immunoprecipitation from murine plasma and cell culture medium

Murine plasma from $PI16^{+/+}$ mice was diluted 1:10 in lysis-buffer before 10 μg of anti-chemerin antibody were added (for the negative control IP antibody was omitted), and the samples were incubated over night at 4 °C in a head-over-toe shaker. 20 μl Protein G resin (Dynabeads, Invitrogen) was added, and the mixture was incubated at room temperature for 2 h while shaking. After three washing steps with PBS, samples were resuspended in denaturing sample buffer, boiled for 10 min, and loaded onto a 15% SDS-polyacrylamide gel. For immunoprecipitation from cell culture medium, 500 μl of the medium was used. After incubation over night at 4 °C with 10 μg anti-PI16

antibody [4], samples were processed similar to the samples of the immunoprecipitation from plasma.

4.5. Western blot analysis

Lysates from tissue or cultured cells were fractionated by SDS-PAGE (8 or 15% polyacyrylamide) and blotted according to standard procedures. Primary antibodies against murine PI16 [4] and murine chemerin (R&D Systems AF2352) were diluted 1:1000, secondary antibodies were anti-rabbit, anti-mouse and anti-goat (diluted 1:10,000 in PBS + 0.5% Tween20). Chemiluminescence was quantified by Multi-Gauge image analysis software (Fujifilm) and normalized to signals of GAPDH protein.

4.6. Immunohistochemistry and immunofluorescence staining

Myocardial tissues from $PI16^{+/+}$ and $PI16^{-/-}$ mice were snapfrozen and fixed with formalin, embedded in paraffin, cut, and stained with haematoxylin and eosin. Immunohistochemistry (IHC) was performed with an automated immunostainer (Discovery® Xt, Roche) using protein A-purified rabbit polyclonal antibody (20 ng/μl) against exon 5-ecoded, purified PI16 peptide. Heat-induced antigen retrieval in 5% EDTA pH 8 buffer was used and Gomori-Masson staining was performed after IHC. To detect PI16 in transfected CHO cells, cells were fixed with 4% paraformaldehyde, incubated with an anti-PI16 antibody (1:100 dilution) and detected by Alexa 568-conjugated anti-rabbit-IgG secondary antibody (Life Technologies). Cells were subsequently embedded in Vectashield (Vector labs) and images were taken with a Leica TCS SP5 Confocal microscope.

4.7. FRET measurements

HEK293 cells were transfected with constructs encoding murine pro-chemerin and PI16-ΔGPI-Fc, and cultured in DMEM/10% FCS. The supernatant was collected 48 h after transfection and transferred onto CMKLR1-sensor cells (HEK293 cells co-transfected with plasmids encoding CMKLR1-CFP and YFP-β-Arrestin2, 48 h previous to treatment with conditioned medium). FRET was measured as previously described [24], using a Zeiss Axio Observer Z1 inverted microscope equipped with DualView2 and an Evolve camera (Photometrics). The emission intensity of CFP (at 480 ± 20 nm) and YFP (at 535 ± 15 nm) were recorded upon excitation at 436 nm using the Metafluor software (Molecular Devices). The recorded YFP signal was corrected for spillover of CFP and data were analysed with Prism 6 (GraphPad Software).

4.8. PI16 purification

Plasmid vectors for fusion constructs of mouse Pi16 and a human IgG Fc fragment (see above for primers and host vectors, and Fig. 3 for schematic drawing) were stably transfected in CHO cells using Lipofectamine 2000 (Life technologies, procedure according to manufacturer). Positive clones were selected by resistance to Zeocin (400 μg/ml; InvivoGen). After positive expression control (on Western blots), 2 l of cell culture medium were collected and passed through 1 ml Protein A resin (HiTrap Protein A HP, GE Healthcare) for approx. 30 h at 4 °C at a flow rate of 1 ml/min. After several washings with 10 ml of 20 mM sodium phosphate, proteins were eluted by 100 mM glycine, pH 3 and immediately neutralized in 500 μl 1 M Tris pH = 8.5. Protein concentration was determined according to absorbance at 280 nm.

4.9. Chemerin ELISA in plasma

Chemerin was quantified in plasma from $PI16^{+/+}$ and $PI16^{-/-}$ mice using the Mouse Chemerin Quantikine ELISA Kit (R&D Systems). 10 μl plasma from heparinized blood were used and processed according to the manufacturer's protocol. Measurement was carried out in a Tecan Infinite 200 multiplate reader at 450 nm with wavelength correction at 540 nm.

4.10. Phospholipase C cleavage assay

HEK293 cells were transiently transfected with a plasmid construct for full-length murine PI16 (using Lipofectamine 2000, Life Technologies). 48 h after transfection, cell-free medium was collected for further analysis and cells were washed with PBS. Thereafter, 0.1 units of phospholipase C (Invitrogen) in PBS was added to the cells and incubated for 20 min at 37 °C. Cells and cell-free supernatants were analysed by SDS-PAGE.

4.11. Protein lysates

Lysates from tissue or from cultured cells were prepared using 2% SDS lysis buffer (50 mM Tris, 1 mM $NaVO_4$, 2% m/v SDS). Frozen tissue was mechanically homogenized in this lysis buffer. After incubation with benzonase (5% (v/v) final concentration), tissues were further distorted by sonification for 10 min. Afterwards, protein concentration was measured by Pierce BCA protein assay (Life Technologies) and diluted to 1 μg/μl in 2% SDS lysis buffer for SDS-PAGE.

4.12. Targeted gene disruption of murine Pi16 locus

The targeting vector for the PI16 locus was designed to target exons 3 and 4 of murine PI16, flanking it with loxP sites for targeted deletion of PI16. The construct was first amplified in bacteria, then linearized and electroporated in embryonic stem cells (ES-cells (Nagy R1 clone, passage 13 [25]). Clones were selected for neomycin resistance (encoded by the targeting construct) and verified by PCR and Southern Blot using the primers forward 5′-GAATTCGATAACTGCAGATATAAC-3′ and reverse 5′-CACAGCGCATACAAGGATGG-3′. The reverse primer was also used as a Southern blot probe. Verified clones were expanded and injected into blastocysts of the SV129 mouse line, leading to chimeric mice that carried the modified *Pi16*-allele in their germ line. After crossing these mice with wildtype C57BL/6N mice, genomic DNA from tail biopsies was screened for insertion of the neomycin targeting cassette using the primers LoxpF 5′-GACAGATTCCATCCTTAAGTCCC-3′ and LoxpR 5′- CCCGGCCACGGGCCCTTCGCAC-3′. A band that corresponds to 249 bp was observed in mice carrying the neomycin cassette, whereas a shorter product (88 bp) was detected in wild-type mice. After crossing $Pi16^{floxneo}$ mice with *Actb*-Flp mice and *nestin*-Cre mice, global genetic deletion of the *Pi16*-exons 3 and 4 was confirmed in a three-primer-PCR (5′flloxp1: 5′- ACCAACCAACCGAATAACCA-3′, LoxpF: 5′-GACAGATTCCATCCTTAAGTCCC-3′, Delloxp4R: 5′- TCCGCTTAGAGG ACTGCCTA-3′) that generated a band of 341 bp in the genetically modified mice and a band of 146 bp in wildtype mice.

4.13. In vitro protease assay

In an assay for cathepsin K activity (BioVision), 0.02 mU recombinant cathepsin K was incubated with 0.01 mM substrate (*Z*-Gly-Pro-Arg-AMC (Peptanova)) with or without the denoted concentrations of purified PI16-ΔGPI-Fc. The assay was carried out in 100 μl (in 50 mM NaOac, pH = 5.5, 2.5 mM EDTA, 1 mM DTT, 0.01% Triton X-100). As a positive control for the inhibition of cathepsin K, E-64 was applied (0.1 mM). Substrate turnover was monitored upon absorbance at 370 nm in a Tecan multiplate reader infinite 200, and normalized to a control without protease inhibitor.

Funding

This work was supported by the Deutsche Forschungsgemeinschaft (DFG FOR923 to S.E.).

Conflict of interest

None declared.

Acknowledgements

We thank Lucia Koblitz, Sabine Brummer and Kornelija Sakac for technical assistance. Furthermore, we thank Yvonne Döring and Manuela Mandl from the IPEK Munich for fruitful discussions on the interaction of chemerin and PI16. PLC cleavage quantification has in part been subject of a masters thesis by S.S.

Appendix A. Supplementary data

Supplementary data to this article can be found online at http://dx.doi.org/10.1016/j.yjmcc.2016.08.010.

References

[1] J.N. Cohn, R. Ferrari, N. Sharpe, Cardiac remodeling - concepts and clinical implications: a consensus paper from an international forum on cardiac remodeling. Behalf of an International Forum on Cardiac Remodeling, J. Am. Coll. Cardiol. 35 (2000) 569–582.
[2] Y. Sassi, A. Ahles, D.J. Truong, Y. Baqi, S. Lee, B. Husse, et al., Cardiac myocyte – secreted cAMP exerts paracrine action via adenosine receptor activation, J. Clin. Invest. 124 (2014) 5385–5397.
[3] A.V. Shinde, N.G. Frangogiannis, Fibroblasts in myocardial infarction: a role in inflammation and repair, J. Mol. Cell. Cardiol. 70 (2014) 74–82.
[4] R.J. Frost, S. Engelhardt, A secretion trap screen in yeast identifies protease inhibitor 16 as a novel antihypertrophic protein secreted from the heart, Circulation 116 (2007) 1768–1775.
[5] J.R. Reeves, J.W. Xuan, K. Arfanis, C. Morin, S.V. Garde, M.T. Ruiz, J.C. Wisniewski, et al., Identification, purification and characterization of a novel human blood protein with binding affinity for prostate secretory protein of 94 amino acids, Biochem. J. 385 (2005) 105–114.
[6] I.C. Nicholson, C. Mavrangelos, D.R.G. Bird, S. Bresatz-Atkins, N.G. Eastaff-Leung, R.H. Grose, et al., PI16 is expressed by a subset of human memory Treg with enhanced migration to CCL17 and CCL20, Cell. Immunol. 275 (2012) 12–18.
[7] T.J. Sadlon, B.G. Wilkinson, S. Pederson, C.Y. Brown, S. Bresatz, T. Gargett, et al., Genome-wide identification of human FOXP3 target genes in natural regulatory T cells, J. Immunol. 185 (2010) 1071–1081.
[8] N. Koshikawa, T. Nakamura, N. Tsuchiya, M. Isaji, H. Yasumitsu, M. Umeda, et al., Purification and identification of a novel and four known serine proteinase inhibitors secreted by human glioblastoma cells, J. Biochem. 119 (1996) 334–339.
[9] K. Bozaoglu, J.E. Curran, C.J. Stocker, M.S. Zaibi, D. Segal, N. Konstantopoulos, et al., Chemerin, a novel adipokine in the regulation of angiogenesis, J. Clin. Endocrinol. Metab. 95 (2010) 2476–2485.
[10] B. Bondue, V. Wittamer, M. Parmentier, Chemerin and its receptors in leukocyte trafficking, inflammation and metabolism, Cytokine Growth Factor Rev. 22 (2011) 331–338.
[11] B.A. Zabel, M. Kwitniewski, M. Banas, K. Zabieglo, K. Murzyn, J. Cichy, Chemerin regulation and role in host defense, Am. J. Clin. Exp. Immunol. 3 (2014) 1–19.
[12] J.L. Cash, R. Hart, A. Russ, J.P.C. Dixon, W.H. Colledge, J. Doran, et al., Synthetic chemerin-derived peptides suppress inflammation through ChemR23, J. Exp. Med. 205 (2008) 767–775.
[13] T. Yoshimura, J.J. Oppenheim, Chemerin reveals its chimeric nature, J. Exp. Med. 205 (2008) 2187–2190.
[14] D. Rodríguez-Penas, S. Feijóo-Bandín, V. García-Rúa, A. Mosquera-Leal, D. Durán, A. Varela, et al., The adipokine chemerin induces apoptosis in cardiomyocytes, Cell. Physiol. Biochem. 37 (2015) 176–192.
[15] O. Zhang, Q. Ji, Y. Lin, Z. Wang, Y. Huang, W. Lu, et al., Circulating chemerin levels elevated in dilated cardiomyopathy patients with overt heart failure, Clin. Chim. Acta 448 (2015) 27–32.
[16] I. Barbaric, G. Miller, T.N. Dear, Appearances can be deceiving: phenotypes of knockout mice, Brief. Funct. Genomic. Proteomic. 6 (2007) 91–103.
[17] B. Eisenhaber, P. Bork, F. Eisenhaber, Sequence properties of GPI-anchored proteins near the omega-site: constraints for the polypeptide binding site of the putative transamidase, Protein Eng. 11 (1998) 1155–1161.
[18] K.B. Goralski, T.C. McCarthy, E.A. Hanniman, B.A. Zabel, E.C. Butcher, S.D. Parlee, et al., Chemerin, a novel adipokine that regulates adipogenesis and adipocyte metabolism, J. Biol. Chem. 282 (2007) 28175–28188.
[19] B.A. Zabel, S.J. Allen, P. Kulig, J.A. Allen, J. Cichy, T.M. Handel, et al., Chemerin activation by serine proteases of the coagulation, fibrinolytic, and inflammatory cascades, J. Biol. Chem. 280 (2005) 34661–34666.
[20] S.R. Alam, D.E. Newby, P.A. Henriksen, Role of the endogenous elastase inhibitor, elafin, in cardiovascular injury: from epithelium to endothelium, Biochem. Pharmacol. 83 (2012) 695–704.
[21] V. Wittamer, J.-D. Franssen, M. Vulcano, J.-F. Mirjolet, E. Le Poul, I. Migeotte, et al., Specific recruitment of antigen-presenting cells by chemerin, a novel processed ligand from human inflammatory fluids, J. Exp. Med. 198 (2003) 977–985.
[22] K. Bozaoglu, K. Bolton, J. McMillan, P. Zimmet, J. Jowett, G.K. Collier, et al., Chemerin is a novel adipokine associated with obesity and metabolic syndrome, Endocrinology 148 (2007) 4687–4694.
[23] G. Iacobellis, Local and systemic effects of the multifaceted epicardial adipose tissue depot, Nat. Rev. Endocrinol. 11 (2015) 363–371.
[24] A. Ahles, F. Rodewald, F. Rochais, M. Bünemann, S. Engelhardt, Interhelical interaction and receptor phosphorylation regulate activation kinetics of different human beta1-adrenoceptor variants, J. Biol. Chem. 290 (2015) 1760–1769.
[25] A. Nagy, J. Rossant, R. Nagy, W. Abramow-Newerly, J.C. Roder, Derivation of completely cell culture-derived mice from early-passage embryonic stem cells, Proc. Natl. Acad. Sci. U. S. A. 90 (1993) 8424–8428.